Diffusion-Controlled Hysteresis

PETER I. RAVIKOVITCH AND ALEXANDER V. NEIMARK*
*Center for Modeling and Characterization of Nanoporous Materials, TRI/Princeton, 601 Prospect Ave.,
Princeton, New Jersey 08542-0625, USA*

ravikovi@triprinceton.org
aneimark@triprinceton.org

Abstract. A new model of time-dependent sorption-desorption hysteresis is presented. This type of hysteresis is not related to transitions between metastable adsorption states, which are a common cause of capillary condensation hysteresis in mesoporous materials. We show that time-dependent hysteresis is a consequence of slow kinetics and failure to reach equilibrium at given experimental conditions. The model of diffusion-controlled hysteresis (DCH) we developed is capable of predicting time-dependent experimental data. It allows one to estimate the characteristic diffusion. We show that DCH model time and the equilibrium sorption isotherms from non-equilibrium sorption/desorption measurements. The DCH model has been tested using experimental CO_2 isotherms on polymeric and carbonaceous materials.

Keywords: sorption, hysteresis, equilibrium, kinetics, diffusion

1. Introduction

Hysteresis between (ad)sorption and desorption branches of the isotherms has been observed for many systems (Everett, 1967; Gregg and Sing, 1982). In this work we discuss the so-called time-dependent sorption-desorption hysteresis (Everett, 1967). This type of hysteresis is not related to the transitions between metastable equilibrium states that is a common cause of permanent capillary condensation hysteresis in mesoporous materials (Everett, 1967; Gelb et al., 1999). For subcritical fluids, time-dependent hysteresis extends below the lower closure point of the capillary condensation hysteresis; it can embrace the entire range of pressures in the case of supercritical fluids. Examples include a broad range of materials, primarily microporous carbons, natural and synthetic polymer fibers and membranes, and geosorbents, such as soil particles (White et al., 1998).

In the literature, time-dependent hysteresis is almost always attributed to deformations of the solid

material during (ad)sorption (Gregg and Sing, 1982). The most prominent example is swelling of smectite clays (Tvardovski et al., 2001). While sorption deformation may be important, we argue that slow transport/diffusion of sorbate molecules can explain, at least semi-quantitatively, specifics of time-dependent hysteresis, including the behavior of scanning hysteresis loops and the maxima on the desorption branch. Earlier attempts to describe the scanning hysteresis loops involved an empirical dynamic model (Park, 2002). In the present work we show that characteristic features of time-dependent hysteresis can be described by a simple diffusion equation.

In what follows, we do not restrict ourselves to any particular system. We show that slow diffusion and failure to reach equilibrium at a given experimental protocol, mainly an insufficiently slow rate of the increase/decrease of the bulk pressure, causes the time-dependent hysteresis in many systems. It is equally applicable to both *adsorption* and *absorption* phenomena. As a first approximation, our model assumes that swelling effects can be neglected. However, the model can be extended to include sorption deformation effects.

---

*To whom correspondence should be addressed.

2. Model

We consider that the solid material consists of two domains, the transport domain and the sorption domain. That is, in order for a molecule to be (ad)sorbed in the sorption domain, it has to travel through the transport domain. In the transport domain, (ad)sorption may occur also, however, it is assumed that the equilibrium concentration in the transport domain is a linear function of the external pressure, as if it would be, for example, in the case of dissolution. Local equilibrium between the two domains is assumed. A Equilibrium is described using a dual-mode isotherm. It includes a nonlinear term to describe equilibrium in the sorption domain and a linear term to describe equilibrium between the bulk fluid (outside of the solid particle) and the fluid in the transport domain:

$$N_w^{eq} = c(p) + a_w(p) \qquad (1)$$

Here $c(p) = K_d p$ and $a_w(p)$ (per unit weight of the solid, in mmol/g) represent concentrations in the transport and sorption domains, respectively; p is the pressure in the bulk fluid phase. For the sake of simplicity we consider that the primary solid particles are spherical of a certain radius R_S. This assumption is not important, and any other geometry can be assumed. For spherical particles, the radial diffusion-sorption model gives:

$$\frac{\partial(c + a(c))}{\partial t} = D\frac{1}{r^2}\frac{\partial}{\partial r}\left(r^2\frac{\partial c}{\partial r}\right) \qquad (2)$$

Here c (mmol/cm^3) is the concentration in the transport domain; $a(c)$ (mmol/cm^3) is the equilibrium concentration in the sorption domain; D (cm^2/s) is the diffusion coefficient. Below we consider subcritical sorption, and it is convenient to rewrite the above equation in terms of the variables that are directly measured in sorption experiments, e.g. relative pressure in the bulk gas phase, $u = p/p_0$, and sorption per unit weight of the particles. To this end, we transit from the concentration, c, to a new dimensionless variable $\tilde{u} = c/(K_d p_0)$:

$$\frac{\partial\tilde{u}}{\partial t} = \frac{D}{1 + \frac{1}{K_d p_0}\frac{da_w(\tilde{u})}{d\tilde{u}}}\frac{1}{r^2}\frac{\partial}{\partial r}\left(r^2\frac{\partial\tilde{u}}{\partial r}\right) \qquad (3)$$

Here $a_w(\tilde{u})$ represents the equilibrium sorption isotherm. The parameters of this equation are: (1) In-

verse characteristic time of diffusion, D/R_S^2; (2) Parameters of the nonlinear adsorption isotherm, $a_w(\tilde{u})$; (3) The Henry constant for the transport domain, K_d. The boundary conditions are:

$$\frac{\partial\tilde{u}}{\partial t}\bigg|_{r=0} = 0 \quad \text{and} \quad \tilde{u}(t)\bigg|_{r=R_S} = u(t) = p(t)/p_0 \qquad (4)$$

The key ingredient of the model is that the time dependence of the pressure/concentration on the grain boundary, $p(t)$, is the function taken from the sorption-desorption experiment. Thus, the boundary condition is determined by the experimental protocol. It is an increasing function during the sorption experiment and a decreasing function during the desorption experiment.

To compare with the experimentally measured nonequilibrium sorption-desorption isotherms, the uptake per unit weight of the solid is calculated as:

$$N_w^{\text{noneq}} = \frac{3}{4\pi R_S^3}\int_0^{R_S} 4\pi r^2(a_w(\tilde{u}) + K_d p_0\tilde{u})dr$$
$$= 3\int_0^1 \left(\frac{r}{R_S}\right)^2 (a_w(\tilde{u}) + K_d p_0\tilde{u})d\left(\frac{r}{R_S}\right) \qquad (5)$$

Different equations can be used to describe the nonlinear sorption term $a_w(p)$ in Eq. (1), for example, the Dubinin-Radushkevich (DR) or Langmuir equations. In its general form, Eq. (3) is a nonlinear partial differential equation, which has to be solved numerically. MATLAB codes for direct (prediction of sorption- desorption isotherms) and reverse (fitting experimental sorption-desorption curves) problems have been developed. The codes have been tested using two analytically solvable problems—linear sorption/diffusion with arbitrary boundary conditions, and linear sorption/diffusion in a semi-infinite media.

3. Examples

3.1. Scanning Hysteresis Loops

In the first example we have simulated the theoretical scanning hysteresis loops (Fig. 1) to demonstrate the main features of DCH sorption. Calculations presented in Fig. 1 were performed with the Langmuir isotherm for the nonlinear adsorption domain: $a_w(u) = a_w K_H u/(a_w + K_H u)$. The parameters were $D/R_S^2 = 0.005$, $a_w = 100$, $K_H = 1$, $K_d = 1$.
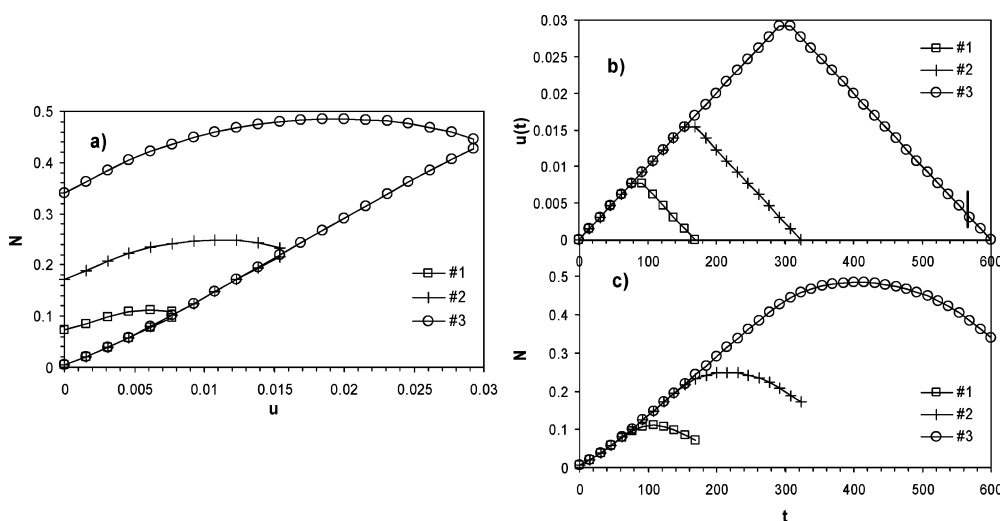
Figure 1. (a) Adsorption isotherm and three desorption scanning isotherms calculated using the DCH model. Time dependences of the (b) bulk pressure and (c) adsorbed phase concentration during adsorption-desorption processes.

Parameters of the model were not optimized to fit any experimental data quantitatively. The model simulated the sorption/desorption process in which the bulk pressure was first increasing linearly with time (sorption) and then decreasing linearly (desorption) (see Fig. 1(b)). This is a slightly simplified version of the real sorption/desorption experiment. In real volumetric or gravimetric static sorption experiments, the increase in the bulk pressure during sorption (decrease during desorption) is step-wise. The straight lines in Fig. 1(b) approximate these step-wise functions. The three lines in Fig. 1(b), denoted by different symbols, correspond to three scanning desorption isotherms, i.e. the desorption process started at three different times ($\sim$300, $\sim$150 and $\sim$80).

Figure 1(c) shows the total sorption uptake Eq. (5) as a function of time. It can be seen that the maxima on the uptake curves always lag behind the maxima on the corresponding bulk pressure curves. This is the main feature of the DCH model. The concentration gradient leads to the inward diffusion that continues for some appreciable period of time even after the driving force (bulk pressure) has been reversed. This is a fingerprint of DCH mechanism. When the total sorption uptake is plotted versus the bulk pressure, one can see typical sorption-desorption hysteresis loops (Fig. 1(a)). When diffusion is slow enough, desorption scanning isotherms may exhibit maxima (Fig. 1(a)). Such maxima clearly indicate that we deal with non-equilibrium sorption.

3.2. Hysteretic Sorption/Dissolution

In the second example we used the DCH model to describe experimental data on carbon dioxide sorption/desorption on a sample of human hair fiber measured at 273 K and pressures up to 1 atm. The measurements were performed with Autosorb-1 volumetric instrument from Quantachrome Corp. The temperature was maintained using an in-house made electric thermostat. Prior to each sorption/desorption run the hair sample was evacuated at 323 K. Two runs were performed in which the interval between two successive sorption/desorption points on the isotherm was $\sim$30 minutes and $\sim$70 minutes, respectively. The first run consisted of 40 sorption and 40 desorption points, and the second run consisted of 40 sorption and 25 desorption points.

Figure 2(a) shows CO_2 uptake as a function of time (like Fig. 1(c) in the previous example). The vertical arrows mark the beginning of desorption. Figure 2(b) shows the sorption/desorption isotherms in standard coordinates of uptake versus pressure of bulk CO_2 at 273 K. The isotherms form very wide hysteresis loops with prominent maxima on the desorption branches. The sorption branches are linear at low pressures with an upward curvature at higher pressures, which is typical for CO_2 dissolution in polymeric materials.

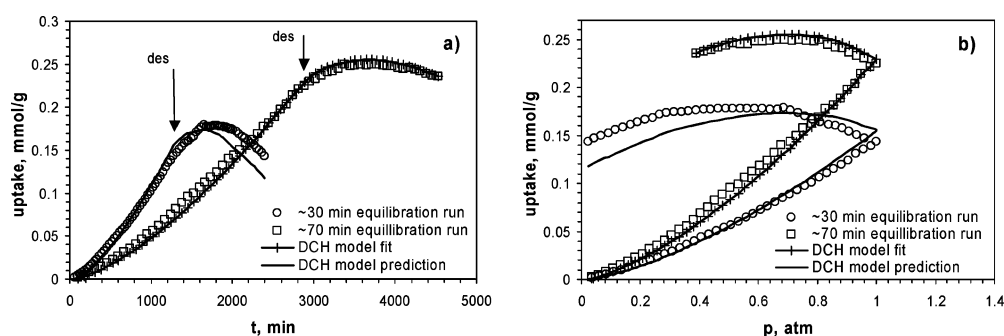The lines in Figs. 2(a) and (b) are the calculated results obtained as follows. The shape of the

Figure 2. Carbon dioxide sorption/desorption on a sample of human hair fiber at 273 K. (a) Uptake as a function of time. (b) Sorption/desorption isotherms as a function of pressure. Circles and squares denote experimental data points for two runs performed with different equilibration times (∼30 and ∼70 minutes). The vertical arrows indocate the time of the beginning of desorption. The data from the ∼70 min run were fitted with the DCH model (lines with crosses) and sorption/desorption for the ∼30 min run was predicted by the model (lines).

sorption branches indicates that we deal with *absorption*/dissolution rather than *adsorption* phenomenon. In this case one can use a linear isotherm to describe the equilibrium between the absorbed and bulk fluids, $N_w^{eq} = K_d p$. It is not necessary to distinguish sorption and transport domains, and the model reduces

to the diffusion equation with two parameters and boundary conditions determined by the experimental sorption/desorption protocol. We fitted the experimental points from the longer (∼70 minutes equilibration time) run and obtained the following two parameters of the model: $D/R_S^2 = 1.06 \times 10^{-4}$ min^{-1}, $K_d =$
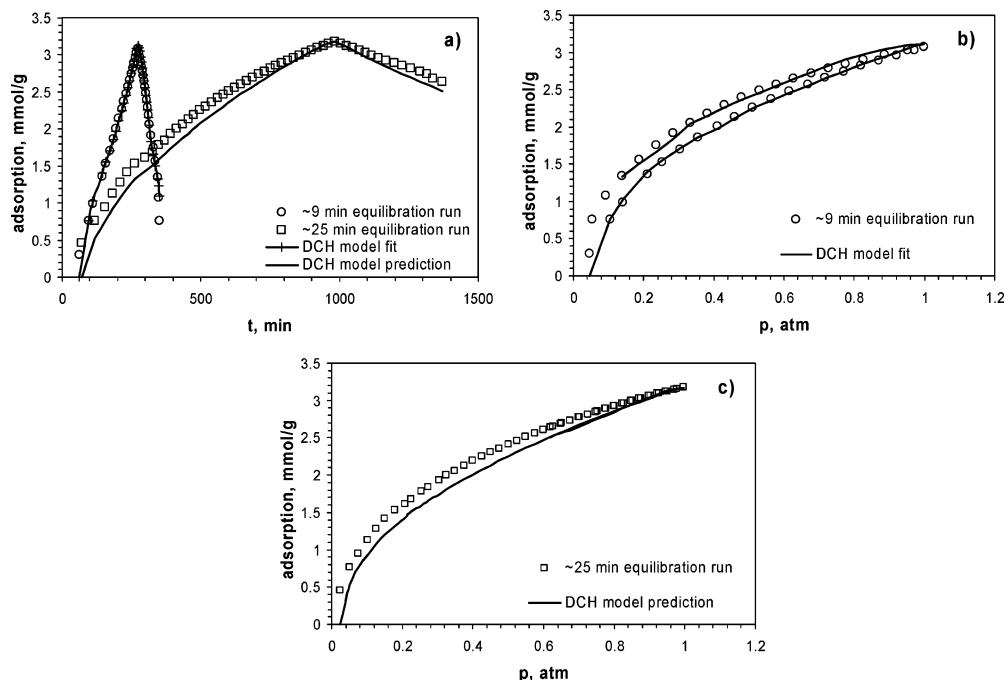

Figure 3. Carbon dioxide adsorption/desorption on microporous CFCMS activated carbon fiber at 273 K. (a) Uptake as a function of time. (b) and (c) Adsorption/desorption isotherms. Circles and squares denote experimental data for two runs with ∼9 and ∼25 minutes equilibration intervals, respectively. The data from ∼9 min run were fitted with the DCH model and the equilibrium adsorption isotherm for ∼25 min run was predicted by the model.

1.37 mmol/g/atm. The mean error of the fit was ∼3 percent. Then, the obtained parameters of the model were used to predict the data from the shorter (∼30 minutes equilibration time) experimental run. As it can be seen from Fig. 2, the model predicted CO_2 uptake for ∼2.3 times shorter sorption/desorption run rather well.

3.3. Adsorption in Micropores

In the third example we consider CO_2 *adsorption* on a sample of microporous carbon fiber composite molecular sieve (CFCMS) (Burchell and Judkins, 1996) (Fig. 3). In this case, the adsorption isotherms are highly nonlinear, in accord with theoretical CO_2 adsorption isotherms in carbon micropores (Ravikovitch et al., 2000). The sample was outgassed at 200°C for 48 hours prior to adsorption measurements. In the first experimental run, we deliberately used short equilibration times (on average ∼9 min per pressure point) to obtain non-equilibrium hysteretic sorption/desorption isotherm. In the second run, we used longer equilibration times (on average ∼25 min per pressure point) and obtained completely reversible adsorption/desorption isotherm (Fig. 3). The data from the first (non-equilibrium) run were fitted with the DCH model, and the data from the second (equilibrium) run were predicted by the model. We used DR equation to describe adsorption in micropores: $a_w(u) = a_w \exp[-(RT/(E\beta)\log(u))^2]$. The parameters of the model were: $D/R_S^2 = 0.037\,\mathrm{min}^{-1}, a_w = 3.78\,\mathrm{mmol/g},$ $E = 31.3$ kJ/mol, and $K_d = 1.06$ mmol/g/atm. The affinity coefficient for CO_2 was taken $\beta = 0.35$ (Garrido et al., 1987). It can be seen that, except for a slight offset in the total amount adsorbed at low pressures, the model was able to predict the equilibrium adsorption isotherms in reasonable agreement with the measured equilibrium data, and to predict the disappearance of the hysteresis loop.

4. Discussion and Conclusions

Our results indicate that the DCH model describes time-dependent sorption-desorption hysteresis loops in different systems. It is quite remarkable that such a simple model is able to predict almost quantitatively rather complex sorption/desorption behavior, including maxima on the desorption isotherms (see e.g. Fig. 2).

We stress that the model is not intended to describe the systems being trapped in a metastable equilibrium state separated from another equilibrium state by a free energy barrier, which is a primary cause of the capillary condensation/desorption hysteresis (Everett, 1967; Neimark et al., 2000). The time scale needed to relax a metastable system toward true equilibrium is much larger than the time scale of diffusion transport/relaxation responsible for the time-dependent hysteresis discussed here.

Despite the success of the present model, we note that slow diffusion of sorbate may not be the sole cause of time-dependent hysteresis. Adsorption may cause volumetric changes of the sorbent (Braida et al., 2003), such as expansion or contraction, which result in a slow relaxation process coupled with sorbate diffusion. In the case of swelling, for example, the total sorption capacity on the desorption path may be larger than the initial sorption capacity. Another mechanism is the so-called conditioning effect, which manifests itself in the fact that subsequent (ad)sorption measurements on the same material tend to give higher sorption uptake (Lu and Pignatello, 2002; Wang et al., 1998). For the CFCMS sample we have found that after we had performed two adsorption runs described above (Fig. 3), subsequent adsorption runs yielded exactly the same equilibrium isotherm, even when short equilibration times were used. One of the explanations for this peculiar behavior is that the solid structure may contain molecular size constrictions, which lead to diffusion/transport limitations during the first adsorption run, but did not affect subsequent runs because of the widening of the pores and/or dissolution of some residual volatile compounds. It is known that CFCMS materials contain some amounts of phenolic resin (Burchell and Judkins, 1996). In fact, hysteretic CO_2 adsorption/desorption behavior has been reported for molecular sieve carbons derived from phenolic resin (Nakashima et al., 1995).

All of the above mechanisms may contribute to the overall adsorption-desorption hysteresis. It should be noted also that the model we presented can be augmented to consider other transport mechanisms occurring during sorption/desorption as well as a more detailed description of diffusion and sorption by including such parameters as porosity, tortuosity, etc. In conclusion, our results indicate that the specifics of time-dependent hysteresis can be described by the model of diffusion-controlled hysteresis, which allows one to assess the characteristic diffusion time and to estimate the equilibrium sorption isotherm from non-equilibrium sorption-desorption measurements.

Acknowledgments

References

Braida, W.J., J.J. Pignatello, Y. Lu, P.I. Ravikovitch, A.V. Neimark, and B. Xing, *Environ. Sci. Technol.*, **37**, 409–417 (2003).

Burchell, T.D. and R.R. Judkins, *Energy Conv. Manag.*, **37**, 947–954 (1996).

Everett, D.H., in *The Solid-Gas Interface*, E.A. Flood (Ed.), Vol. 2. Marcel Dekker, New York, 1967.

Garrido, J., A. Linares-Solano, J.M. Martin-Martinez, M. Molina-Sabio, F. Rodriguez-Reinoso, and R. Torregrosa, *Langmuir*, **3**, 76–81 (1987).

Gelb, L.D., K.E. Gubbins, R. Radhakrishnan, and M. Sliwinska-Bartkowiak, *Rep. Prog. Phys.*, **62**, 1573–1659 (1999).

Gregg, S.J. and K.S.W. Sing, *Adsorption, Surface Area and Porosity*; Academic Press, New York, 1982.

Lu, Y.F. and J.J. Pignatello, *Environ. Sci. Technol.*, **36**, 4553–4561 (2002).

Nakashima, M., S. Shimada, M. Inagaki, and T.A. Centeno, *Carbon*, **33**, 1301–1306 (1995).

Neimark, A.V., P.I. Ravikovitch, and A. Vishnyakov, *Phys. Rev. E*, **62**, R1493-R1496 (2000).

Park, I. in *Fundamentals of Adsorption 7*, K.K.H. Kaneko and Y. Hanzawa (Eds.), pp. 991–998, IK INternational, Chiba-City, Japan, 2002.

Ravikovitch, P.I., A. Vishnyakov, R. Russo, and A.V. Neimark, *Langmuir*, **16**, 2311–2320 (2000).

Tvardovski, A.V., A.A. Fomkin, Y.I. Tarasevich, and A.I. Zhukova, *J. Colloid Interface Sci.*, **241**, 297–301 (2001).

Wang, J.S., Y. Kamiya, and Y. Naito, *J. Polym. Sci. Pt. B-Polym. Phys.*, **36**, 1695–1702 (1998).

White, J.C., P.I. Ravikovitch, R. Russo, A.V. Neimark, and J.J. Pignatello, in *1996–1998 Bioremediation Research Program Review: EPA/600/R-89/122*, pp. 19–20, U.S. Environmental Protection Agency, Washington, DC, 1998.